Building a Cargo Aircraft's Vertical Fin Blade with Structural Steel, E-Glass, and Carbon Fiber: A Finite Element Comparison and Design Study

PERUGU ANIL KUMAR[1], Dr.P. RAVIKANTH RAJU[2], Dr.B. SANDHYA RANI[3]
[1]PG Student, CAD/CAM, Ellenki College of Engineering and Technology.
[2]Assoc Prof., Department of Mechanical Engineering, Ellenki College of Engineering and Technology.
[3]Head of the Dept., Department of Mechanical Engineering, Ellenki College of Engineering and Technology.

To Cite this Article
Perugu Anil Kumar, Dr. P. Ravikanth Raju, Dr. B. Sandhya Rani, "Building a Cargo Aircraft's Vertical Fin Blade with Structural Steel, E-Glass, and Carbon Fiber: A Finite Element Comparison and Design Study", Journal of Science Engineering Technology and Management Science, Vol. 03, Issue 07, July 2026, pp: 1077-1085, DOI: http://doi.org/10.64771/jsetms.2026.v03.i07.pp1077-1085
Submitted: 20-06-2026 *Accepted: 25-07-2026* *Published: 31-07-2026*

Abstract - Because it is cantilevered from the fuselage tailcone, the vertical fin (also known as a vertical stabilizer) must be as lightweight as possible while nevertheless being large enough to support significant bending and shear loads in order to maintain the aircraft's directional (yaw) stability. Comparing the structural performance of three candidate materials structural steel, E-glass fiber, and carbon fiber (230 GPa grade) under an identical static side-load case, this paper presents the design, 3D solid modeling, and finite element structural analysis of a representative fin blade assembly for a cargo aeroplane. Under a uniformly distributed 0.5 MPa pressure load and with a fixed-support boundary condition at the root fitting, the fin geometry—which includes a primary fin box, spar, and lower ventral fairing—was modeled in CATIA V5 and studied in ANSYS Workbench. Total deformation was 0.471 mm and peak von Mises stress was 48.16 MPa for structural steel, while mass was highest for E-glass fiber at about one-third the density of steel. The highest deformation was 4.066 mm for carbon fiber, which was modeled using dry, fibers-only orthotropic properties and had an unfavourable fiber orientation relative to the fin load path, as well as pronounced transverse compliance. By all accounts, the three materials did not deviate from their elastic limit values. The findings suggest that E-glass fiber provides a safe alternative to steel in terms of weight reduction when using the simplified material models that were considered. However, it is anticipated that a carbon fiber reinforced polymer structure that is correctly laminated and optimized for weight reduction will offer the most significant weight savings, pending additional orthotropic laminate analysis.

Index Terms - Topics covered include: cargo aircraft, static structural analysis, E-glass fiber, carbon fiber, empennage, vertical fins, and fin blades.

I. INTRODUCTION

A typical fixed-wing aircraft's empennage, with its horizontal and vertical stabilizers, offers both longitudinal and directional stability. Cantilevered from the fuselage tailcone, the fin blade is the principal load-carrying box of the vertical stabilizer. It requires it to respond to rudder-manoeuvre loads, engine-out (asymmetric thrust) stresses at minimum control speed (VMC), and lateral gust loads. The fin blade is made up of spars, ribs, and a stressed skin. Fins are a good choice for comparing materials because, in multi-engine cargo aircraft, the VMC situation after the main engine fails often dictates rudder and fin size [3, 4].

Removing weight from the empennage, which is at the very back of the plane, improves fuel economy and the aircraft's center of gravity more than a similar reduction closer to the center of gravity would. This is why this study sets out to systematically compare two composite systems—E-glass and carbon fiber—with structural steel, a traditional metallic material.

ISSN:3049-0952
www.jsetms.com

Comparing structural steel, E-glass fiber, and carbon fiber (230 GPa grade) under an identical representative side-load case, this paper presents the design, solid modeling, and static structural finite element analysis of a representative fin blade for a cargo aeroplane. CATIA V5 is used for geometry, and ANSYS Workbench is used for finite element analysis.

II. LITERATURE REVIEW

In the past, preliminary sizing of tapered, sweeping lifting-surface structures like the fin box was done using early, hand-calculation-based methods [1]-[3]. These methods relied on load scenarios, sizing philosophy, and closed-form beam-theory idealizations. For the rudder-deflection and engine-out load scenarios that dictate fin size, Etkin and Reid [4] provide the stability-and-control foundation. Kassapoglou [5], Jones [6], and Peters [12] provide thorough treatments of composite structural behavior and the orthotropic elastic response of fiber-reinforced materials. Zienkiewicz et al. [7] present the finite element formulation that lies beneath the discretization, assembly, and solution procedure utilized in ANSYS Mechanical [8].

Several previous publications have used CAD/FEA procedures similar to this one to analyze empennage components. In their analysis of aircraft vertical stabilizers using ANSYS Workbench, Athreya [13] compared candidates made of aluminum, silicon carbide, and titanium alloy under static structural loading. They found results that were similar to the current study's metallic-versus-lightweight-alternative comparison in terms of stress and strength-to-weight ratio. Dong [16] also demonstrated, for flexural loading, that the stacking sequence and fiber mix of carbon/glass hybrid laminates strongly govern stiffness and strength outcomes, reinforcing that dry, single-orientation fiber properties are not indicative of an engineered laminate. Thianwiboon [14] utilized ANSYS ACP to optimize a hybrid carbon/glass composite empennage afterbody laminate, which goes to show that a correctly stacked, multi-ply hybrid laminate can significantly surpass either constituent fiber system when used alone. This finding is directly relevant to the fibers-only modeling limitation discussed in Section V. Modern finite element modeling has a wider use, as shown by Vladimirescu et al. [15], which evaluates the structural and vibration aspects of an operational aircraft as they pertain to the empennage. Unfortunately, no prior research has filled the particular need by contrasting an isotropic metallic baseline with an isotropic-equivalent glass fiber and an orthotropic carbon fiber system on a single fin blade geometry. This study does so under a common load situation and employs a CATIA-to-ANSYS process.

When it comes to designing main airframe components, the commercial and cargo aerospace industry relies on CATIA, a computer-aided three-dimensional interactive application [9]. The platform's Generative Shape Design tools work wonders with the tapered, swept outer mould lines that are typical of empennage surfaces. EASA CS-25 [10] and FAA 14 CFR Part 25 [11] describe certification-level fin and rudder load cases; this research, unlike Section VI, employs a single sample static load case instead of the whole certification envelope.

III. METHODOLOGY

A. The Shape of a Fin Blade

A twin- or multi-engine cargo aircraft's fin blade shape resembles a sweeping, tapered vertical stabilizer box. This box has the fin root, an outside aerodynamic skin, and an interior spar structure. The tailcone of the fuselage is integrated with the lower ventral fairing extension. The main geometric and load characteristics are summarized in Table I.

Parameter	Value / Description
Overall fin height (root to tip)	≈ 1200 mm
Root chord (incl. ventral fairing)	≈ 2000 mm
Planform	Swept, tapered
Internal structure	Main spar with stiffening web, stressed outer skin
Root boundary condition	Fixed support at root attachment fitting
Applied load	Uniform 0.5 MPa pressure on aerodynamic surface

Table I. Primary Geometric and Load Parameters of Fin Blades

B. Potential Ingredients

Three potential materials were chosen from among the many metallic and composite options for fin construction: structural steel, which is dense and strong; E-glass fiber, which is inexpensive and has the same properties as glass; and carbon fiber, which is highly orthotropic and has high fiber-direction stiffness. The mechanical characteristics used are detailed in Table II and were sourced from the ANSYS Engineering Data material library. As mentioned in Section V, the dry, "fibres only" qualities are represented by E-glass and carbon fiber, respectively. These materials do not include the resin matrix of a cured laminate.

Property	Steel	E-Glass	Carbon (230 GPa)
Density (kg/mm³)	$7.85 \times 10^{-[illegible]}$	$2.6 \times 10^{-[illegible]}$	$1.8 \times 10^{-[illegible]}$
Elasticity type	Isotropic	Isotropic	Orthotropic
E, fibre/X (MPa)	200,000	73,000	230,000
E, transverse/Y (MPa)	—	—	23,000
Poisson's ratio (XY)	0.30	0.22	0.20
Yield / Ultimate (MPa)	250 / 460	n/s (fibres only)	n/s (fibres only)

The table Chapter II. Potential Material Characteristics (ANSYS Engineering Data)

C. Finite Element Modeling and Solid Modeling

The fin blade solid model was created in CATIA V5 using the following tools: the Part Design and Generative Shape Design workbenches for parts and shapes, the Pad and Rib features for the main fin box and its components (including the spar web), the lower ventral fairing extension for sections, and a root attachment fitting for the boundary condition face. I used the native CATIA-to-ANSYS geometry interface to import the finished CATPart into ANSYS Workbench. Then, I used the default tetrahedral mesh generation in Workbench, which is based on curvature and proximity, and I applied local refinement at the leading edge and fillet transitions.

The effectively rigid confinement of the fuselage tailcone frame was represented by a fixed-support boundary condition at the root attachment fitting, and an extreme side-gust or rudder-hinge-moment-induced loading condition was represented by a uniformly distributed 0.5 MPa pressure load on the aerodynamic surface of the fin. In order to ensure a like-for-like comparison, a static structural solution was performed individually for each of the three candidate materials. Each run yielded the total deformation, equivalent elastic strain, and equivalent (von Mises) stress fields. The Engineering Data cell was the only cell that was updated.

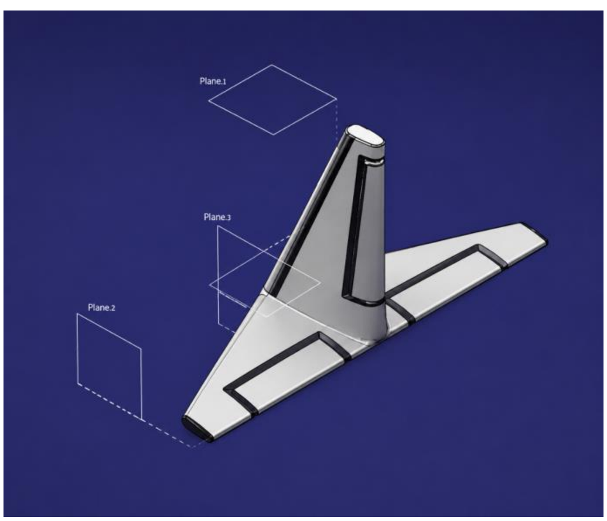

Fig. 1. An assembly of fin blades rendered in CATIA V5 solid form.

ISSN:3049-0952
www.jsetms.com

Fig. 2. Solid model of a fin blade with several perspectives.

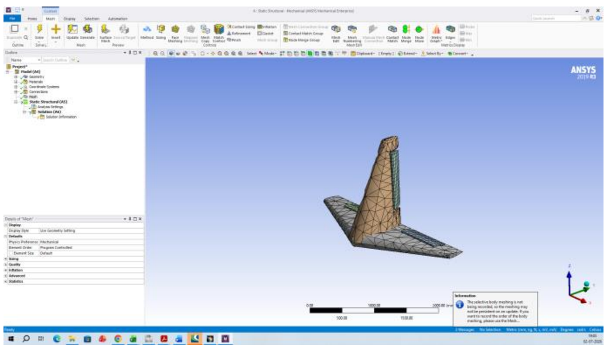

Fig. 3. Final assembly of the fin blades (including the primary fin housing, spar, and inferior ventral fairing) finite element model.

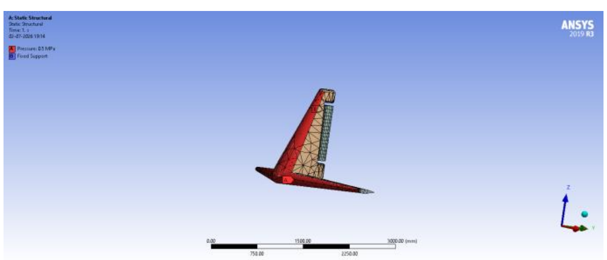

Fig. 4. The aerodynamic surface must be subjected to a consistent pressure load of 0.5 MPa and a fixed support (B) at the root attachment fitting are the boundary requirements.

IV. RESULTS

Here we summarize the numerical comparisons made after presenting the ANSYS Mechanical contour findings (total deformation, equivalent elastic strain, and equivalent (von Mises) stress) for all the candidate materials obtained under the load situation specified in Section III-C.

A. Reinforced Metal

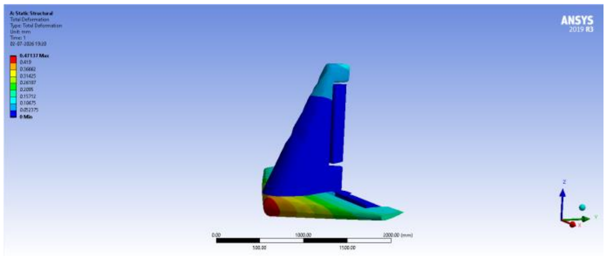

Fig. 5. The structural steel's total deformation contour cannot exceed 0.4714 mm.

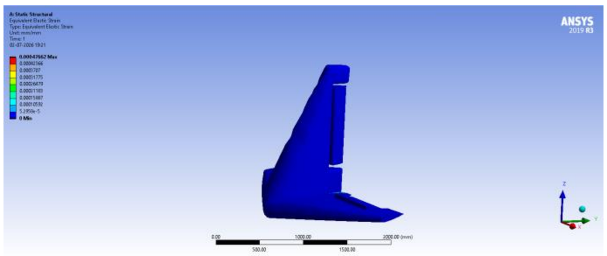

Fig. 6. Structural steel with an equivalent elastic strain contour (maximum 4.766×10^{-4} mm/mm).

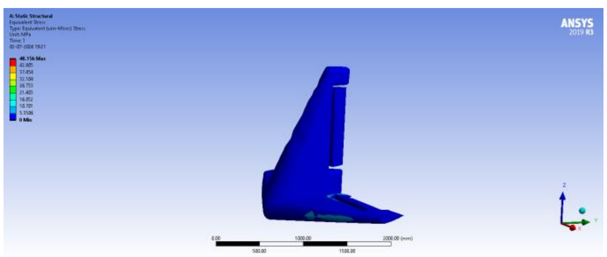

Fig. 7. Similar stress profile for structural steel (up to 48.16 MPa), as determined by von Mises analysis.

In the lower, loaded area of the fin box next to the ventral fairing, distortion and stress are at their highest. A notional safety factor of around 5.2 is provided by the peak stress of 48.16 MPa in comparison to the 250 MPa yield strength.

B. Energy-Glass Fiber

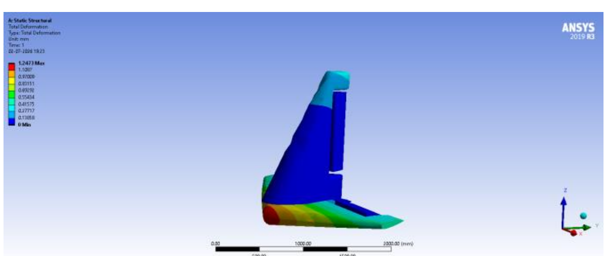

Fig. 8. The maximum thickness of the deformation contour for E-glass fiber is 1.2473 mm.

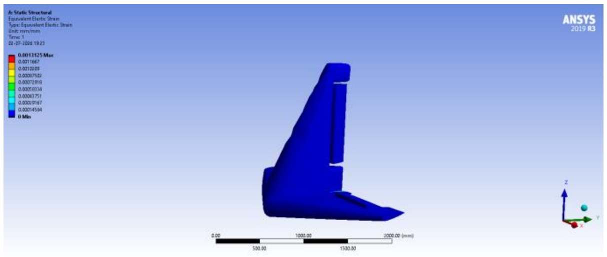

Fig. 9. This is the E-glass fiber equivalent strain contour, with a maximum value of 1.313×10^{-3} mm/mm.

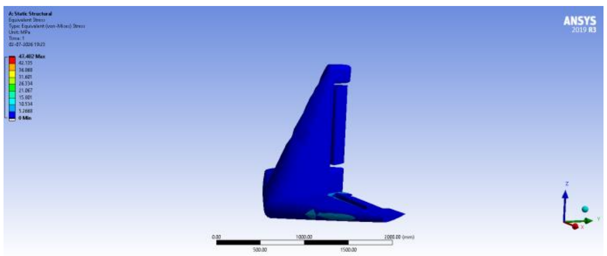

Fig. 10. With an equivalent stress contour of E-glass fiber, the maximum allowable strain is 47.40 MPa.

Peak stress (47.40 MPa) stays about the same as in the steel case, but deformation rises to 1.247 mm (≈ 2.6 times the steel value), in line with E-glass's lower modulus.

C. Grade 230 GPa Carbon Fibre

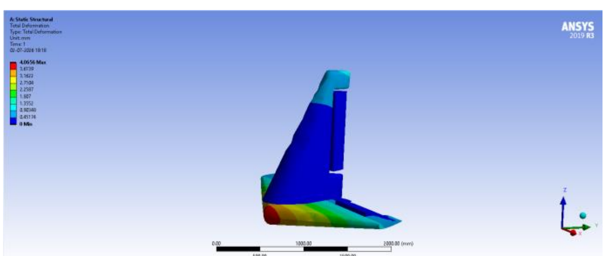

Fig. 11. Contour of total deformation for carbon fiber (maximum 4.0656 mm).

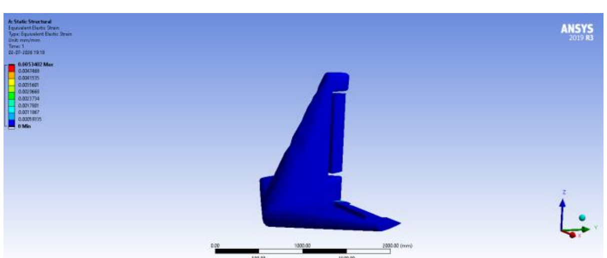

Fig. 12. An elastic strain contour with a maximum value of 5.340×10^{-3} mm/mm is equivalent to carbon fiber.

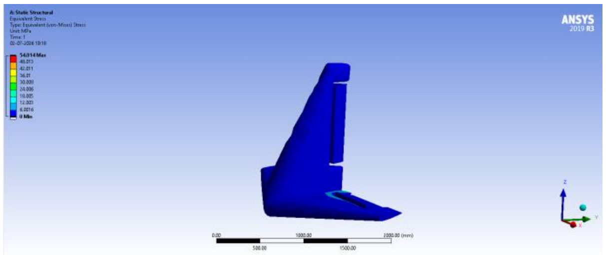

Fig. 13. Corresponding stress profile for carbon fiber (maximum 54.01 MPa; von Mises equivalent).

Carbon fiber has the largest fibre-direction modulus of the three possibilities, at 230,000 MPa, but it also has the most deformation, at 4.066 mm, as discussed in Section V. Peak stress, at 54.01 MPa, is comparable to the other two materials.

D. Combined Evaluation

Table III summarizes the ANSYS Mechanical findings of all three candidate materials and their related mass fractions relative to the steel baseline.

Material	Deform. Max (mm)	Strain Max (mm/mm)	Stress Max (MPa)	Mass (% of steel)
Structural Steel	0.4714	4.766 × 10^− [illegible]	48.16	100
E-Glass Fibre	1.2473	1.313 × 10^− [illegible]	47.40	≈33
Carbon Fibre (230 GPa)	4.0656	5.340 × 10^− [illegible]	54.01	≈23

The table III. Mixed Finite Element Findings, All Potential Substrates

The boundary-condition interpretation was constant throughout all three runs, with the highest deformation and stress recorded in the lower, pressure-loaded fin box area close to the ventral fairing, and a subsequent decrease toward the fixed-support root (see Figs. 5, 8, and 11).

V. DISCUSSION

Since carbon fiber has a higher fiber-direction modulus (230,000 MPa) than steel and E-glass, the result for carbon fiber seems paradoxical at first glance. This simplified single-orientation model does not account for the fact that the load-carrying skin and spar surfaces of the fin are not aligned with the fiber's stiff direction, and that the transverse modulus of the fibers-only material model is lower than that of E-glass (73,000 MPa). Instead of the nominal 230 GPa figure, the material's relatively flexible transverse and shear characteristics regulate the effective stiffness that controls the deflection response of the fin. Thianwiboon [14] and Dong [16] showed that for hybrid carbon/glass laminates, the resin matrix provides the shear-transfer mechanism between plies, allowing a multi-ply laminate to approach a near-quasi-isotropic in-plane stiffness; this is not the case for actual carbon-fiber-reinforced polymer fins. This finding should not be interpreted as proof that carbon fiber is structurally inferior for fin assembly, but rather as a lower-bound indication of the repercussions of bad fiber-orientation design.

In accordance with the classical linear-elasticity result, which states that the stress field in a linear-elastic body under prescribed loading and boundary conditions is mainly governed by geometry, differing between materials mainly through the (here modest) variation in Poisson's ratio, and that deformation is directly governed by stiffness, the relatively narrow spread of peak stress across the three materials (47-54 MPa) is acceptable.

To evaluate the structural adequacy of the composite candidates, a full laminate analysis using a suitable composite failure criterion (e.g., Tsai-Wu or Hashin) would be necessary, since neither candidate could be found in the material library that was used. This would have prevented a safety-factor assessment similar to that done for steel. Dynamic (flutter) and fatigue behavior, which is especially relevant to a rudder-carrying flight-control surface, were outside the present linear-static scope, and the single representative static side-load case that was examined does not reflect the fuller, multi-case rudder-manoeuvre, engine-out, and gust load envelope that is required for certification-level substantiation under EASA CS-25 [10] or FAA Part 25 [11].

Thus, according to the simplified material models used here, E-glass fiber provides a safe and beneficial weight reduction compared to steel. However, according to the orthotropic laminate analysis that will be conducted in subsequent work, the most promising material family for weight reduction would be a carbon-fiber-reinforced polymer structure with fiber orientations designed to match the principal bending and shear load paths of the fin.

VI. CONCLUSION

For this study, we used CATIA V5 to model a typical cargo plane fin blade and ANSYS Workbench to test three potential materials in a standard static side-load scenario. As a result of its extreme orthotropy and unfavourable fiber orientation rather than any inherent structural inferiority, dry-fiber carbon (230 GPa) caused the greatest deformation (4.066 mm) at approximately 23% of the steel mass, while structural steel had the lowest deformation (0.471 mm) and stress (48.16 MPa) but the greatest mass. E-glass fiber produced an intermediate deformation of 1.247 mm at approximately one-third of the steel mass. When subjected to the stress, none of the three materials deviated from their elastic limit states. We find that E-glass fiber has the best stiffness-to-weight trade-off out of all the simplified material models we looked at. Moving forward, we propose a fully laminated, fiber-optimized carbon-fibre-reinforced polymer design as our top priority. We also need to expand our analysis to include the entire certification load envelope and do dynamic (flutter and fatigue) testing.

REFERENCES

[1] E. F. Bruhn, Analysis and Design of Flight Vehicle Structures. Cincinnati, OH: Jacobs Publishing, 1973.

[2] M. C. Y. Niu, Airframe Structural Design: Practical Design Information and Data on Aircraft Structures. Hong Kong: Conmilit Press, 1988.

[3] T. H. G. Megson, Aircraft Structures for Engineering Students, 6th ed. Oxford, U.K.: Butterworth-Heinemann, 2017.

[4] B. Etkin and L. D. Reid, Dynamics of Flight: Stability and Control, 3rd ed. New York, NY: John Wiley & Sons, 1996.

[5] C. Kassapoglou, Design and Analysis of Composite Structures: With Applications to Aerospace Structures, 2nd ed. Chichester, U.K.: John Wiley & Sons, 2013.

[6] R. M. Jones, Mechanics of Composite Materials, 2nd ed. Philadelphia, PA: Taylor & Francis, 1999.

[7] O. C. Zienkiewicz, R. L. Taylor, and J. Z. Zhu, The Finite Element Method: Its Basis and Fundamentals, 7th ed. Oxford, U.K.: Butterworth-Heinemann, 2013.

[8] ANSYS, Inc., ANSYS Mechanical User's Guide, Release 2019 R3. Canonsburg, PA: ANSYS, Inc., 2019.

[9] Dassault Systèmes, CATIA V5 Part Design and Generative Shape Design User Guides. Vélizy-Villacoublay, France: Dassault Systèmes, 2020.

[10] European Union Aviation Safety Agency (EASA), Certification Specifications and Acceptable Means of Compliance for Large Aeroplanes (CS-25). Cologne, Germany: EASA, 2023.

[11] Federal Aviation Administration (FAA), 14 CFR Part 25 – Airworthiness Standards: Transport Category Airplanes. Washington, DC: FAA, 2023.

[12] S. T. Peters, Ed., Handbook of Composites, 2nd ed. New York, NY: Springer, 1998.

[13] Athreya, “Modelling and finite element analysis of aircraft vertical stabilizer,” Int. J. Res. (IJR), vol. 5, no. 18, 2018.

[14] M. Thianwiboon, “Optimization of a hybrid carbon/glass composites afterbody of the amphibious plane with finite element analysis,” Eng. J., vol. 23, no. 5, pp. 125–140, Sep. 2019.

[15] T. Vladimirescu, I. Fuiorea, and T. Vladimirescu-Jr., “Free vibrations analysis of the aircraft IAR-99 HAWK based on a new and modern finite element model,” INCAS Bulletin, vol. 16, no. 3, pp. 123–132, 2024.